SEMIAUTOMATIC ROAD EXTRACTION BY DYNAMIC PROGRAMMING OPTIMISATION IN THE OBJECT SPACE: SINGLE IMAGE CASE

A. P. Dal Poz[a, *], R. A. Gallis[b], J. F. C. da Silva[a]

[a] Dept. of Cartography, São Paulo State University, R. Roberto Simonsen, 305, Presidente Prudente-SP, Brazil, (aluir, jfcsilva@fct.unesp.br)
[b] Ph.D. Student in Cartographic Sciences, São Paulo State University, R. Roberto Simonsen, 305, Presidente Prudente-SP, Brazil, rodrigogallis@pos.prudente.unesp.br

Commission III

ABSTRACT:

This article proposes a novel road extraction methodology from digital images. The innovation is based on the dynamic programming (DP) algorithm to carry out the optimisation process in the object space, instead of doing it in the image space such as the DP traditional methodologies. Road features are traced in the object space, which implies that a rigorous mathematical model is necessary to be established between image and object space points. It is required that the operator measures a few seed points in the image space to describe sparsely and coarsely the roads, which must be transformed into the object space to make possible the initialisation of the DP optimisation process. Although the methodology can operate in different modes (mono-plotting or stereo-plotting), and with several image types, including multisensor images, this paper presents details of our single image methodology, along with the experimental results.

1. INTRODUCTION

Road extraction from aerial and satellite imagery is of fundamental importance in the context of spatial data capturing and updating for GIS applications. Substantial work on road extraction has been accomplished since the 70's in computer vision and digital photogrammetry, with pioneering works by, e. g., Bajcsy and Tavakoli (1976) and Quam (1978). This research topic is still challenging, what is demonstrate, for example, by the fact that vendors of commercial photogrammetric system have not provided useful toolkits for automated road extraction, including practical semiautomatic ones.

The mentioned classification of the road extraction methods is related to the amount of automation incorporated by them. Semiautomatic methods depend on the intervention of an operator for identifying the road object and supplying a little information about it, as e.g. seed points. These methods include road-follower (McKeown and Denlinger, 1988; Vosselman and de Knecht, 1995; Dal Poz and Silva, 2002; Kim et al., 2004) and some kind of simultaneous curve fitting (Kass et al., 1987; Grüen and Li, 1997; Agouris et al., 2000; Hu et al., 2004; Merlet and Zerubia, 1996; Dal Poz and Vale, 2003). Automated methods try to completely circumvent human intervention during the extraction process. A sophisticated example is found in Baumgartner et al. (1999), in which different resolutions, grouping, and context are used to extract road networks from high-resolution images. Stoica et al. (2004) modelled the road network in remote sensed images as connected line segments, resulting in a probabilistic model to be solved by the Maximum a Posteriori (MAP) estimation. As a final example, Zhu et al. (2004) extracted linear features from laser data and used them to guide the road extraction from aerial images.

While such fully, or at least close to fully, automated processes have not reached a mature state, semiautomatic methods need to be developed or improved to allow the rapid, reliable and accurate provision of data for GIS systems. This article proposes a novel road extraction methodology from digital images. The innovation is based on the dynamic programming optimisation (DP) algorithm to carry out the optimisation process in the object space, instead of doing it in the image space such as the DP traditional methodologies. This paper is organised in four main sections. Section 2 presents our object space road extraction methodology using a single aerial image and a DTM. Results are presented and discussed in Section 3. Finally, conclusions are provided in Section 4.

2. OBJECT SPACE ROAD EXTRACTION USING A SINGLE IMAGE

2.1 Image space road models

Photometric and geometric road properties (as e.g. road is elongated and lighter than the background, road grey levels do not change much within a short distance, road is smooth etc.) are used to formulate a generic road model considering that the road can be represented by an image space polygon $P' = \{p_1, ..., p_n\}$, where p_i is its ith vertex. The generic road model can be formulated by the merit function (equation 1) and an inequality constraint (equation 2), as follows (Gruen and Li, 1997),

$$E = \sum_{i=1}^{n-1} ((E_{p_1}(p_i, p_{i+1}) - \beta.E_{p_2}(p_i, p_{i+1}) + \gamma.E_{p_3}(p_i, p_{i+1})).[1 + \cos(\alpha_i - \alpha_{i+1})]/|\Delta s_i|) \quad (1)$$

$$C_i = |\alpha_i - \alpha_{i+1}| < T \quad (2)$$

---

[*] Corresponding author.

where, $E_{p_1}(p_i, p_{i+1})$, $E_{p_2}(p_i, p_{i+1})$, and $E_{p_3}(p_i, p_{i+1})$ are functions describing geometric and radiometric road properties and depending on consecutive points p_i and p_{i+1}; α_i is the direction of the vector defined by points p_{i-1} and p_i; β and γ are positive constants; $|\Delta S_i|$ is the distance between points p_{i-1} and p_i; and T is a user-defined threshold for direction change between two adjacent vectors.

Analysing the merit function (equation 1), it is easily concluded that the function E is a sum of sub-functions E_i depending only on three consecutive points (p_{i-1}, p_i, p_{i+1}) of the polygon P^i, i.e,

$$E = \sum_{i=1}^{n-1} E_i(p_{i-1}, p_i, p_{i+1}) \qquad (3)$$

Due to the structure of equation 3, where only six variables are interrelated simultaneously, the DP algorithm can be used to efficiently solve the optimisation process, which is transformed into a sequential decision-making process (Gruen and Li, 1997). The solution of this problem is a 2D polygon $P^i = \{p_1, ..., p_n\}$ representing a user-selected road and corresponding to the maximum of merit function E. This function is appropriate to be used in semiautomatic road extraction process from low-resolution images (road widths ranging from 1 to 3 pixels). Mainly in high-resolution images roads usually manifest as wide and homogeneous ribbons. As a result, the extracted polygons would hardly represent the corresponding road axes. In order to avoid this problem, Dal Poz and Vale (2003) proposed an improvement in equation 3. Basically, an edge constraint term was added to the original merit function, resulting in a function (equation 4) that is a sum of sub-functions E_i^t. Each sub-function depends only on three consecutive points (p_{i-1}, p_i, p_{i+1}) of the polygon P^i and respective road widths (w_{i-1}, w_i, w_{i+1}).

$$E^m = \sum_{i-1}^{n-1} E_i^t(p_{i-1}, p_i, p_{i+1}, w_{i-1}, w_i, w_{i+1}) \qquad (4)$$

Equation 4 shows that the goal of the optimisation process by the DP algorithm is similar to the one based on equation 3. The basic difference is that the optimisation process should provide the polygon $P^i = \{p_1, ..., p_n\}$ representing the road centreline and the road widths at the respective vertices. Equation 4 also shows that 9 variable are interrelated simultaneously.

2.2 Object space road model

As shown before, the image space road model has as unknowns the image co-ordinates (L, C) of polygon vertices representing the road and, in case of high-resolution images, the road width for every polygon vertex as well. Equation 3 or 4 can be modified in order to express roads in function of ground co-ordinates. The resulting equation will be the basis for an optimisation problem by the DP algorithm. As a result, it needs to have an appropriate structure, like one of equation 3 or 4, thus allowing the DP algorithm to be advantageous for solving the optimisation problem. We show below that a merit function with these characteristics can be easily derived.

We start below with the modification of the equation 3. The basic prerequisite to work in this direction is the selection of the object space reference system in which the 3D vertices of polygons representing roads are referred to. UTM (Universe Transverse Macerator) co-ordinates (E, N) plus the ellipsoidal

height (h) is adopted as the ground reference system. Although this reference system (E, N, h) is not cartesian, it is well-known that a mathematical relation between an object point (P(E, N, h)) referred to it and the corresponding point in the image reference system (p(L, C)) can be established rigorously. In order to establish this mathematical relation, many parameters are needed to be known, like the interior and exterior orientation parameters of the sensor, the datum and UTM map projection parameters, beside others.

For frame camera images, the relation between an image space point $p_i(L_i, C_i)$ and the corresponding object space point $P_i(E_i, N_i, h_i)$ can be established in function of known parameters, such as usual ones listed below:

- λ_{cm} is the longitude of the central meridian of a UTM fuse;
- a and f_e are respectively the semi major axis and the flattening of the ellipsoid;
- ϕ_0, λ_0, and h_0 are the geodetic co-ordinates (ϕ_0, λ_0) and the ellipsoidal height (h_0) of the origin of the local vertical reference system;
- κ, φ, ω, X_0, Y_0, and Z_0 are the exterior orientation parameters of the camera, previously computed by an orientation procedure, taking as reference the local vertical reference system;
- f is the focal length of the camera;
- x_0 and y_0 are the co-ordinates of the principal point;
- K_1, K_2, and K_3 are the parameters of radial lens distortions;
- P_1 and P_2 are the parameters of decentering lens distortions;
- ε_{45} is a refraction coefficient for a standard atmosphere, depending upon the flying height above mean sea level and the orthometric height of the object point P_i.

The mathematical relation that allows the transformation from object point $P_i(E_i, N_i, h_i)$ into image point $p_i(L_i, C_i)$ is too complex to be presented here. In fact, it involves object space reference system transformations, projective transformation by the collinearity equations, image space reference system transformations, and introduction of systematic errors to the computed image space points. In addition, mathematical concepts and formulae are well-known. Assuming that L_i and C_i image co-ordinates can be obtained from E_i, N_i, and h_i object co-ordinates by f_1 and f_2 equations, respectively, we have,

$$\begin{aligned} L_i &= f_1(Par, V_i) \\ C_i &= f_2(Par, V_i) \end{aligned} \qquad (5)$$

where Par = (λ_{mc}, a, f_e, ϕ_0, λ_0, h_0, κ, φ, ω, X_0, Y_0, Z_0, f, x_0, y_0, K_1, K_2, K_3, P_1, P_2, ε_{45}) and $V_i = (E_i, N_i, h_i)$. Since Par is known, an image space point can be expressed as a function of only V_i, i. e.:

$$p_i(L_i, C_i) = p_i(f_1(V_i), f_2(V_i)) = p_i(f_1(E_i, N_i, h_i), f_2(E_i, N_i, h_i)) \qquad (6)$$

Expression 6 allows equation 3 to be rewritten as follows,

$$E = \sum_{i=1}^{n-1} E_i(p_{i-1}(L_{i-1}, C_{i-1}), p_i(L_i, C_i), p_{i+1}(L_{i+1}, C_{i+1})) =$$

$$\sum_{i=1}^{n-1} E_i(p_{i-1}(f_1(E_{i-1}, N_{i-1}, h_{i-1}), f_2(E_{i-1}, N_{i-1}, h_{i-1})),$$

$$p_i(f_1(E_i, N_i, h_i), f_2(E_i, N_i, h_i)),$$

$$p_{i+1}(f_1(E_{i+1}, N_{i+1}, h_{i+1}), f_2(E_{i+1}, N_{i+1}, h_{i+1}))) \qquad (7)$$

Equation 7 shows that it depends simultaneously on co-ordinates of three successive object points of a polygon representing a road in the object space, i.e.: $P_{i-1}(E_{i-1}, N_{i-1}, h_{i-1})$, $P_i(E_i, N_i\ h_i)$ e $P_{i+1}(E_{i+1}, N_{i+1}, h_{i+1})$. This means that equation 7 may be rewritten in the following way,

$$E = \sum_{i=1}^{n-1} E_i (P_{i-1}(E_{i-1}, N_{i-1}, h_{i-1}), P_i(E_i, N_i, h_i),$$
$$P_{i+1}(E_{i+1}, N_{i+1}, h_{i+1})) \quad (8)$$

Equation 8 is ambiguous as in principle the energy value E can be the same for infinite object space polygons $P^o = \{P_1, ..., P_n\}$. This is a direct consequence of the well-known characteristic of the transformation given by equation 5, by which one can select infinite object points that map to the same image point. Consequently, equation 8 can not be used for extracting roads without imposing constraints to remove its ambiguity. This ambiguity can be removed if a DTM is available as roads can be enforced to lay on the DTM. This constraint takes the form $h_i = f(E_i, N_i)$, allowing equation 8 to be rewritten as follows,

$$E = \sum_{i=1}^{n-1} E_1 (P_{i-1}(E_{i-1}, N_{i-1}), P_i(E_i, N_i), P_{i+1}(E_{i+1}, N_{i+1})) \quad (9)$$

The maximum of the energy E corresponds to a road runs on the DTM (figure 1), which can be efficiently found by the DP algorithm. Equation 9 shows that only six variables are interrelated simultaneously, implying a similar computational complexity when compared to the corresponding image space equation (equation 3). Equation 9 is the basis for road centreline extraction in the object space using a single low-resolution aerial image. In case of medium- and high-resolution aerial images, it is easily demonstrated that, starting from equation 4, the following equation form can be obtained,

$$E = \sum_{i=1}^{n-1} E_1 (P_{i-1}(E_{i-1}, N_{i-1}), P_i(E_i, N_i), P_{i+1}(E_{i+1}, N_{i+1}),$$
$$W_{i-1}, W_i, W_{i+1}) \quad (10)$$

where, W_{i-1}, W_i, and W_{i+1} are the road widths at points P_{i-1}, P_i, and P_{i+1}, respectively. During the optimisation procedure by DP, object space road widths are sampled and the corresponding values in the image space are required for enforcing the edge constraint. This means that a mathematical relation between image and object space widths is necessary. This mathematical relation can be approximately stated by means of the relation between the local image scale and road widths in both spaces. A rigorous mathematical relation can be also stated, but the approximate relation is efficient and very attractive under the computational viewpoint. This relation is efficient because it needs only to discretize the image space road widths within intervals that contain the optimal road widths. However, a rigorous computation of the object space road widths from the corresponding ones optimised in the image space would require the rigorous projection of road width segments onto the DTM, which is a well-known procedure.

Equations 9 and 10 are the bases for road extraction in the object space using a single aerial image. As commented before, these equations can be modified for other sensors. In this case, it is necessary to adapt equation 5 in accordance with sensor geometry. The solution of equation 9 or 10 by the DP optimisation can be compared to a mono-plotting process proposed by Makarovic (1973). This approach is based on two basic steps: 1- feature digitalisation in the image space; and 2- feature projection onto the DTM by the so-called inverse collinearity equations. In the proposed approach the road features are directly extracted in the object space. As illustrated in figure 1, the road is tracked on the DTM while useful photometric information are searched along roads in the image space. While in Makarovic's approach two well-defined mapping steps (i.e., feature extraction from an image and feature projection onto DTM) can be identified, in our approach both steps are accomplished simultaneously.
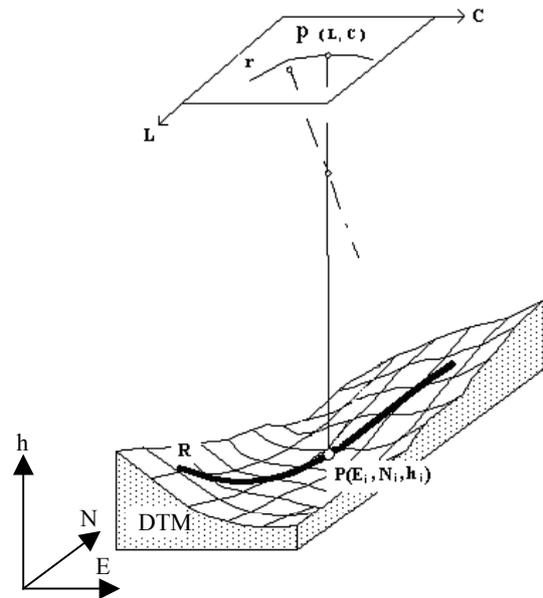

Figure 1. Principle for road extraction in object space

2.3 Strategy for DP optimisation

When in an optimisation problem the variables of the merit function are not interrelated simultaneously, the efficient manner for solving the problem is by applying the DP technique (Ballard and Brown, 1982). Equations 9 and 10 show a structure that meets that requirement, since they have respectively six and nine variables interrelated simultaneously. Below we present only the general strategy developed for extracting 3D polygons representing road centrelines in the object space using the DP algorithm. Mathematical foundations and algorithm aspects can be found in an extensive literature, as e.g. in Ballard and Brown (1982).
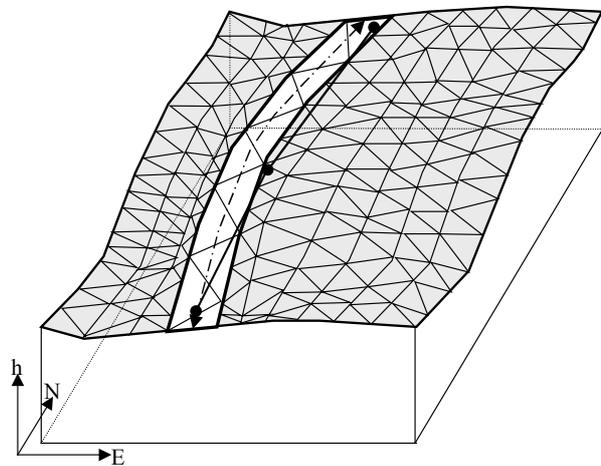

Figure 2. Initialisation of the DP optimisation

No matter what the strategy is used to initialise the proposed methodology, the necessary information are seed points in the reference system where roads will be extracted. Figure 2 shows an illustrative example where three seed points in E, N, and h co-ordinates are used to coarsely describe a road centreline segment. The terrain surface is modelled by a polyhedral model obtained from a regular or irregular mesh. The seed points are collected on or transformed onto the polyhedron, just because the roads will be traced on it.

Figure 3 shows the principle of DP optimisation. Basically, it starts with an initial 3D polygon defined by the user-supplied seed points (black dots in figure 3), which is progressively made dense and refined. In order to accomplish the first iteration, new equidistant vertices are linearly interpolated between every adjacent seed points. In illustrative example of figure 3 two new vertices (marked as circumference) are added. The resulting initial polygon is the reference for generating a search space composed by candidate polygons to accurately represent the road centreline. During the DP optimisation, every vertex may move around its initial position, generating a finite number of polygons. If m is the number of positions each vertex can take and n is the number of vertices defining each polygon, there will be m^n polygons in search space. This means that m should be as small as possible to avoid a prohibitive search space. In order to meet this requirement, the candidates for each best vertex are searched on the polyhedron in direction perpendicular to the actual polygon at each vertex. At the beginning of the optimisation process (i.e., at first iteration) the actual polygon is the initial one. For other iterations, the actual polygon is the one optimised at the last iteration. Figure 3 shows how the search windows are defined at the actual polygon vertices. Each search window is defined as the intersection between the polyhedron and the vertical plane that is perpendicular to the actual polygon at a given vertex. The intersection between each vertical plane and the plane h= 0 is a straight line segment, along which N and E co-ordinates are mathematically interrelated according to equation N= a.E + b, where a and b are the angular and linear coefficient of the straight line, respectively. Now remember that the constraint needed to remove the ambiguity of equation 8 takes the form h= f(E, N) and that the adopted terrain surface model is a polyhedron, the h co-ordinate can be mathematically expressed only in function of E co-ordinate, i.e.,

$$h = A.E + B.(a.E + b) + C \qquad (11)$$

where, A, B, and C are plane coefficients of a polyhedron face. Equation 11 shows that the search windows' points can be sampled by only sampling their E co-ordinate. Two other components are computed internally. In our scheme E co-ordinates are sampled on the plane h= 0 in a such way that the resulting points (E, N= a.E+b) are equally spaced. If the selected distance between sampled points (E, N) is d, E co-ordinates must be sampled such that $|E_{i+1}-E_i| = d/\sqrt{a^2 + 1}$ or $|E_{i+1}-E_i| = d$ for vertical straight lines. Corresponding points (E, N, h) in the search window are not equally spaced due to the varying slope. The advantage of using this strategy is the elimination of the variables N and h, remaining only 3 simultaneous variable (E_{i-1}, E_i, E_{i+1}) in equation 9 or 6 $(E_{i-1}, E_i, E_{i+1}, W_{i-1}, W_i, W_{i+1})$ in equation 10. The drawback is that it does not work for horizontal road segments. However, a small rotation of the search window showed to be efficient to overcome that problem. The value of d is directly related to the resolution, size, and number of elements of the search window. Larger pull-in-range can be obtained by using low-resolution (larger d) and large-sized search windows at first iterations of the optimisation process. An iteration consists of adding new interpolated points to the polygon optimised at the last iteration and of applying to the resulting polygon a new DP optimisation. At last iterations high-resolution and small-sized search windows are used. This strategy allows the computational effort to be reduced properly. During each iteration, two curvature constraints are used to additionally reduce the computational effort. They consist in checking if the horizontal and vertical angles at each polygon vertices are below a given threshold. In order words, only smooth polygons are evaluated by the DP optimisation algorithm. Figure 3 shows that after first iteration the initial polygon is geometrically refined, but it does not accurately described the road centreline. Final result is obtained after checking the convergence of the optimisation process and it is expected to accurately represent the road centreline. Convergence checking consists in verifying after each iteration if all added points are collinear to neighbour points. When this condition is verified, the optimisation process is stopped.
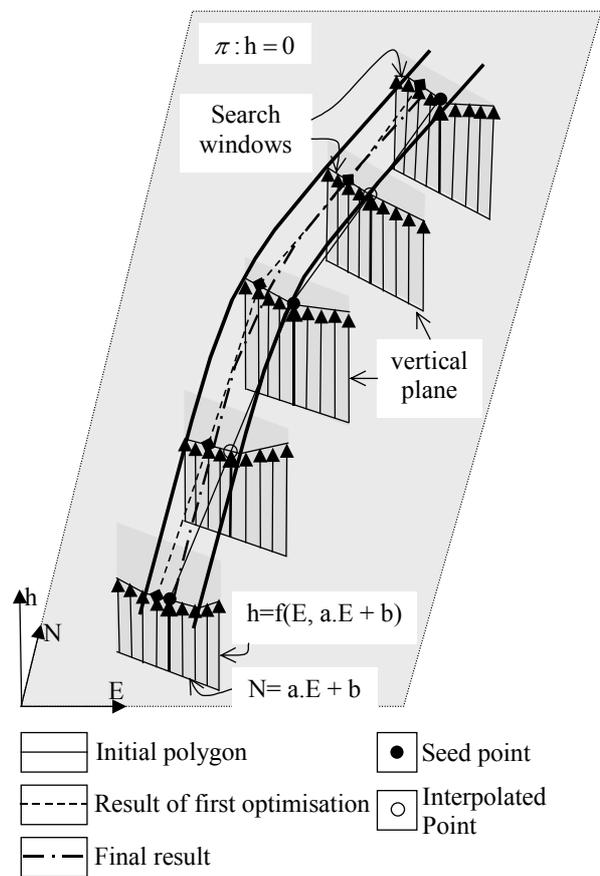

Figure 3. Optimisation strategy

3. RESULTS

The proposed methodology was implemented using Borland C++ Builder 5 compiler for Windows XP. An image (9286 x 9496 pixels) at the approximate scale of 1:9200 is used in experiments (figure 4). This is a high-resolution image, since the pixel footprint is about 26 cm. This image is from a region of Switzerland and is available in the LPS (Leica Photogrammetry Suite®) system, along with the interior and exterior orientation parameters. DTM used in our experiments has a resolution of 5 m.

In order to initialise the road extraction methodology, a few seed points are measured along roads on the image and backprojected onto DTM. Resulting points are seed points needed to start the extraction of each road. Extracted roads in 3D by the DP algorithm are projected into the image reference system (L, C) and overlaid on the input image. This allows a visual analysis of the geometric quality of the extracted road centrelines. Since the methodology depends on some information measured on the image, it is also possible to analyse its robustness against irregularities in the image content, like road obstructions from trees and shadows. Due to the high resolution of the test image, we present below only three selected windows (figures 5, 6, and 7) of it.
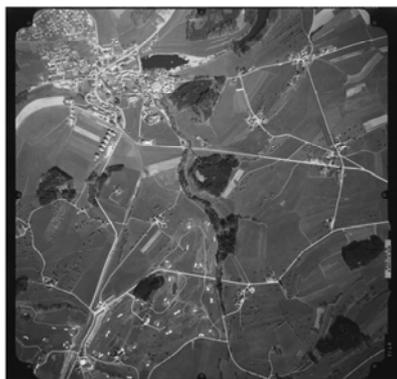

Figure 4. Aerial image used in the experiments

Figure 5 shows the first window where segments of a main road and secondary roads are presented. The results show that the extracted polygons are accurately positioned along the road axes. This is observed even at the road crossings along the main road, where some deficiencies could be expected. An important factor to extract accurate road centrelines is the existence of well-defined road edges, because it allows the edge constraint to be very effective. Places like road crossings, where one or both edges are not presented, can be extracted without deficiencies due to the global curvature constraint enforced in the merit function used in the DP optimisation. This geometric constraint imposes that the accumulate curvature along a road is minimum, implying smoothness to the extracted road centreline. As a result, a short segment of a road affected by some small anomalies (e.g., missing edges at road crossing or obstructions) tend to be represented after extraction by a road centreline segment that has similar curvature to adjacent ones. Although the secondary roads do not have a good contrast with adjacent regions, the road centrelines are accurately extracted.

Figure 6 shows the results in the second window selected in the original image. This example shows two concurrent segments of road, one being straight and another being curved. Both roads have good contrast with adjacent regions and well-defined edges. As in previous example, no significative displacement of road centrelines is observed along the road crossing region. Since for this type of road crossing both edges of each road are missed, the edge constraint almost vanishes. The effect can be better observed on the curved road, where the road centreline segment going through the road crossing region is straight. In general, both road centrelines are accurate, but they show a slight displacement in some parts of road centrelines.

Figure 6. Results in the second window

Figure 7 shows the third window where a curly segment of a road is presented. Even though the contrast of the road with backgrounds is good, some irregularities are visible along and close to the left road curve. The perspective obstruction from the house is very small, but it perturbed a little the extraction process. It is clearly observed that the road centreline changes direction slightly where the house is located. Consequently, along this road segment the extracted road centreline forms a corner and is closer to a road edge. The perspective obstruction caused by trees seems to be not critical to the extraction process. It is also possible to observe the tendency of the road centreline in approaching the internal road edge along road curves. This effect has been commonly observed in other tests. The possible cause is the global curvature constraint enforced in the merit function, by which the accumulate curvature along whole road centreline is minimum. In other words, that global constraint tends to slightly dominate local constraints (e.g., edge constraint). However, irregularities along road curves can disturb the result.

Figure 5. Results in the first window

Figure 7. Results in the third window

In order to access the accuracy of the proposed methodology, road centrelines were manually extracted and compared to corresponding ones extracted by the road extraction algorithm. The node positions of road centrelines were determined to be about 1.3 m in average from the manually extracted road centrelines. This accuracy corresponds to approximately one-sixth of the main roads' mean width.

4. CONCLUSIONS

In this paper was proposed an object space road extraction methodology from a single image. It allowed the integration of two basic steps of data capturing for GIS system, i.e., the road extraction in the image space and the transformation of road features into a map projection. Different resolution aerial images can be handled by the proposed methodology. Terrain information in form of a polyhedron is also necessary to allow the solution of the extraction problem. In order to initialise the extraction procedure, a few seed points is necessary to be supplied on the polyhedron. We identify these points on the image and project them onto polyhedron.

In order to evaluate the methodology one experiment was carried out using a high-resolution aerial image. The results obtained were projected into image space and overlaid on the input image. Three image windows are selected in the input image to analyse the performance of the methodology. In general, the methodology proved to be robust, since it handled irregularities like obstructions. The accuracy of extracted road centrelines is good, although some slight displacements are observed.

Our future works on this subject may include the improvement of the proposed methodology, the development of the multiple image mode, and the development of new application. A possible improvement of the proposed methodology can be accomplished in the merit function. For example, a property not modelled in the merit function (equation 9 or 10) is the smoothness of the road centreline profile in the object space. It is also well-known that asphalt material has very low radiometric responses for laser scanner sensor, property that could be also modelled in the merit function. Consequently, these modifications would allow the integration of laser scanner data with image data for road extraction using DP optimisation. This integration could be carried out both in single image and multiple image modes. An interesting application of the single image methodology is in the refinement of pre-existing road database at smaller scale. In this case, the methodology can be initialised automatically by using pre-existing 3D roads as the first approximation for the DP optimisation.

REFERENCES

Agouris, P., Gyftakis, S., Stefanidis, A., 2000. Uncertainty in image-based change detection (snakes). In: *Accuracy 2000*, Amsterdam, pp. 1-8.

Bajcsy, R., Tavakoli, M., 1976. Computer Recognition of Roads from Satellite Pictures. *IEEE Transaction on System, Man and Cybernetic*, 6(9), pp. 76-84.

Ballard, D. H., Brown, C. M., 1982. *Computer Vision*. Englewood Cliffs, New Jersey: Prentice Hall, 523p.

Baumgartner, A., Steger, C. Mayer, H., Eckstein, W., Ebner, H., 1999. Automatic Road Extraction Based on Multi-Scale, Grouping, and Context. *Photogrammetric Engineering and Remote Sensing*, 66(7), pp. 777-785.

Dal Poz, A. P., Silva, M. A. O., 2002. Active Testing and Edge Analysis for Road Centreline Extraction. In: *The International Archives of the Photogrammetry, Remote Sensing and Spatial Information Sciences*, Graz, Vol. 34, pp. 44-47.

Dal Poz, A. P., Vale, G. M., 2003. Dynamic programming approach for semi-automated road extraction from medium- and high- resolution images. In: *The International Archives of the Photogrammetry, Remote Sensing and Spatial Information Sciences*, Munich, Vol. 34, pp. 87-91, 2003.

Gruen, A., Li, H., 1997. Semi-automatic linear feature extraction by dynamic programming and LSB-snakes. *Photogrammetric Engineering and Remote Sensing*, 63(8), pp. 985-995.

HU, X.; ZHANG, Z.; TAO, C. V. A Robust Method for Semi-Automatic Extraction of Road Centerlines Using a Piecewise Parabolic Model and Least Square Template Matching. Photogrammetric Engineering and Remote Sensing, v. 70, n. 12, 2004, pp. 1393-1398.

Kass, M., Witkin, A. Terzopoulos, D., 1987. Snakes: Active contour models. In: *First International Conference on Computer Vision*, London, UK, pp. 259-268.

Kim, T., Park, S. R., Kim, M. G., Jeong, S., Kim, K. O., 2004. Tracking Road Centerlines from High Resolution Remote Sensing Images by Least Squares Correlation Matching. *Photogrammetric Engineering and Remote Sensing*, 70(12), pp. 1417-1422.

Makarovic, B., 1973. Digital mono-plotters. *ITC Journal*, pp. 583-599.

McKeown, D. M., Denlinger, J. L., 1988. Cooperative methods for road tracking in aerial imagery. In: *Workshop of Computer Vision and Pattern Recognition*, pp. 662-672.

Merlet, N., Zerubia, J., 1996. New prospects in line detection by dynamic programming. *IEEE Transaction on Pattern Analysis and Machine Intelligence*, 18(4), pp. 426-431.

Quam, L. H., 1978. Road Tracking and Anomaly Detection in Aerial Imagery. In: *Image Understanding Workshop*, London, pp. 51-55.

Stoica, R., Descombes, X., Zerubia, J., 2004. *A* Gibbs Point Process for Road Extraction from Remotely Sensed Images. *International Journal of Computer Vision*, 57(2), pp. 121-136.

Vosselman, G., de Knecht, J., 1995. Road tracing by profile matching and Kalman filtering. In: *Automatic Extraction of Man-Made Objects from Aerial and Space Images*, Birkhaeuser Verlag, pp. 265-274.

Zhu, P., Lu, Z., Chen, X., Honda, K., Eiumnoh, A., 2004. Extraction of City Roads Through Shadow Path Reconstruction Using Laser Data. *Photogrammetric Engineering and Remote Sensing*, 70(12), pp. 1433-1440.